International Journal of High Speed Electronics and Systems
Vol. 14, No. 3 (2004) 664–669

World Scientific
www.worldscientific.com

NOISE AND THZ RECTIFICATION CHARACTERISTICS OF ZERO-BIAS QUANTUM TUNNELING SB-HETEROSTRUCTURE DIODES

ARTTU LUUKANEN[¶]*
ERICH N. GROSSMAN[§]
National Institute of Standards and Technology[†]
325 Broadway, Boulder, CO 80305, USA
[¶] *luukanen@boulder.nist.gov*
[§] *grossman@boulder.nist.gov*

HARRIS P. MOYER[♯]
JOEL N. SCHULMAN [♠]
HRL Laboratories LLC, 3011 Malibu Canyon Road, Malibu CA 90265-4797, USA
[♯] *hpmoyer@hrl.com*
[♠] *schulman@hrl.com*

The Sb-heterostructure quantum tunneling diode, fabricated from epitaxial layers of InAs and AlGaSb, is a recently proposed device for direct detection and mixing in the submillimeter wavelength range. These diodes exhibit especially high curvature in the current-voltage characteristic that produces the rectification or mixing without bias. Operation without bias is a highly desirable feature as the device does not suffer from large $1/f$ noise, a major shortcoming in other devices such as Schottky barrier diodes or resistive room temperature bolometers. In this paper we present the noise characteristics of the diode as a function of the bias voltage. At room temperature and zero bias, the device demonstrates a Johnson noise limited intrinsic noise equivalent power of 1 pW/Hz$^{1/2}$. In addition to the noise measurements, we present the detection characteristics of the diode at a frequency of 2.5 THz. The measured THz laser response deviates from conventional theoretical prediction based on pure rectification. The reasons for the discrepancy will be discussed.

*On leave from VTT Information Technology, Espoo, Finland
†Contribution of U.S. Government, not subject to copyright in the U.S.

1. Introduction

At present, millimeter-wave imaging focal-plane arrays are based on microwave monolithic integrated circuits (MMICs), and their pixel count is limited by the complexity and cost of the components and assembly [1]. Moreover, the maximum operation frequency is limited by the availability of low noise amplifiers to $\lesssim$ 200 GHz. Bolometers can provide a low cost alternative and cover frequencies up to the infrared, albeit with lower sensitivity [2,3,4]. Schottky diodes, the workhorse technology for high frequency mixers, can also operate as direct detectors up to several THz, though they typically display an RC-limited rolloff above a few hundred GHz. Their great drawback has been $1/f$ noise, brought about by the DC bias required for sufficient curvature of the IV curve.

In this paper we present the $1/f$ noise performance of a recently introduced direct detector, the InAs/AlSb/GaSb heterostructure backward diode [5,6,7]. The principle of operation is similar to that of an Esaki tunnel diode in that the controlling current mechanism is interband tunneling between adjacent energetically offset semiconductor regions. For low Al concentrations, the Type II band gap line-up between InAs and AlGaSb, in which the conduction band minimum of InAs lies energetically below the valence band maximum of AlGaSb, creates a natural asymmetry in the current flow with bias direction. The special feature of these diodes is that they exhibit highly non-linear IV characteristics near zero bias. In the ideal case, the absence of DC bias means that the devices do not suffer from $1/f$ noise. These merits combined suggest that the quantum tunneling diodes can provide an attractive choice for large integrated millimeter-wave imaging arrays of the future.

2. Diode IV measurements

The InAs/AlSb/GaSb tunnel diode layers are deposited using molecular beam epitaxy on semi-insulating GaAs substrates, using an InAs buffer layer process, identical to that described in Ref. 8. The InAs layer is followed by a 200 nm thick GaSb anode, 20 nm of undoped AlGaSb, a 3.2 nm thick undoped AlSb tunnel barrier, a 50 nm thick InAs cathode, and finally an n^+ InAs contact layer.

Three nominally-identical diodes with a junction area of 2 μm $\times$ 2 μm were characterized by first measuring their DC IV characteristics, while monitoring the differential conductance dI/dV and its derivative d^2I/dV^2 using a lock-in technique. A 100 Hz excitation voltage $V_{osc} = 10$ mV was superimposed on the DC bias voltage through a transformer coupled to the diode bias circuit. The resulting AC voltage across a series resistor, R_L, was connected through a low-noise preamplifier with a gain of 100 to the lock-in input. The measured IV and dI/dV are shown in Fig 1. a. At $V = 0$, the three diodes had a mean junction resistance of $\overline{R}_j$ = (14.4 $\pm$ 0.1 kΩ). The current responsivity (or curvature) of the diode is given by $\gamma = (d^2I/dV^2)/(dI/dV)$, and for the three measured diodes we obtained a mean curvature of -39.5 A/W at zero bias. A measured $\gamma(V)$ for one diode is shown in Fig. 1 b. The divergences at 43 mV and at 111 mV correspond to the points where

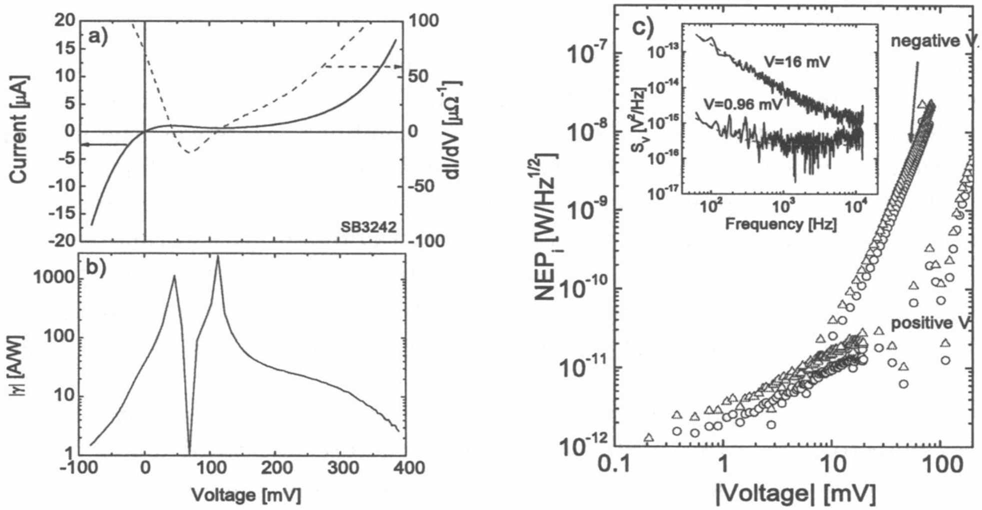

Fig. 1. a) The IV characteristics (solid line) of the diode with the dI/dV curve (dashed line) as a function of the bias voltage. b) The absolute value of current responsivity $\gamma(V)$. c) The matched (circles) and unmatched (triangles) NEP of a diode as a function of the absolute value of dc bias. The minimum NEP is obtained at $V = 0$ due to the rapid increase in $1/f$ noise which overcomes the increase in the responsivity at small positive bias. The inset shows noise spectra recorded at V=0.96 mV and V=16 mV. The dashed lines indicate the fits to the spectra.

dI/dV crosses zero.

3. Noise measurements

IV measurements, combined with noise characterization, determine the true figure of merit for a direct detector, the noise equivalent power (NEP). The diode was again biased in series with the 10 kΩ current sensing resistor, R_L, using a programmable battery power supply. A low-noise preamplifier with a gain of 100 and an input equivalent noise floor of 1.5 nV/$\sqrt{\text{Hz}}$ was used to amplify the voltage noise fluctuations across the current sensing resistor. The output of the preamplifier was connected to a spectrum analyzer, and noise spectra were recorded at different bias voltages in a frequency band from 62 Hz to 12.5 kHz. As the rectified RF power produces a small positive DC voltage across the device, we concentrate on the noise at positive bias. Two representative noise spectra are shown in the inset of Fig. 1 c. At $V = 0$ the noise corresponds to the Johnson noise of the junction resistance R_j. At finite values of V the $1/f$ and current shot noise appear. To quantify the $1/f$ noise, each spectrum was fit with a voltage noise power spectral density given by $S_{\text{fit}} = \alpha V^m/f^r + v_n^2$, where the white noise term v_n includes contributions from the Johnson noise and the shot noise. For the three diodes, the mean fitted values yielded $\alpha = 3.18 \cdot 10^{-6}$ Volts^{2-m}Hz^{r-1}, $m = 2.58$ and $r = 1.33$. Even though the

$1/f$ noise does not directly affect the NEP at zero bias, we note that it does have an effect on the dynamic range of the device.

The origin of the $1/f$ noise in our diodes is likely due to a similar scenario as that described in Ref. 9, according to which thermally excited traps states modulate the barrier height and thus its transmission coefficient. Whether the noise arises from the bulk of the device or is associated with surface states can be determined by measuring the $1/f$ noise properties of diodes with different junction area, and is a subject of future work.

In the following discussion of the NEP, a typical diode small signal circuit is used, with a resistance, R_s, in series with the parallel combination of R_j and C_j. The values for the circuit parameters are from earlier network analyzer and numerical modeling results with $R_s = 17.6\ \Omega$ and $C_j = 13.6$ fF. A noteworthy property of the tunnel diodes is that C_j is only weakly dependent of bias voltage [10]. The intrinsic NEP of the diode across a pre-detection bandwidth $\Delta\omega$ can be calculated from $\mathrm{NEP}_i = \sqrt{S_V/\mathcal{R}_{V0}^2}$, where $\mathcal{R}_{V0} = R_j\gamma/2\{(1 + R_s/R_j)[1 + R_s/R_j + R_sR_jC_j^2(\Delta\omega^2/4 + 3\omega_c^2)/3]\}$ is the average voltage responsivity around a center frequency ω_c for the case of a matched source impedance (e.g. the antenna) and infinite load impedance [11]. Considering first the zero bandwidth case ($\Delta\omega = 0$), when operated at zero bias, and at $\omega_c/2\pi \gg (R_jR_sC_j^2)^{-1/2} \approx 23$ GHz, the voltage responsivity yields with the given junction parameters $\mathcal{R}_{V0} \approx 16\,000$ V/W [12], with the noise given by the Johnson noise of R_j yielding $\mathrm{NEP}_i|_{\Delta\omega=0} \approx \sqrt{16k_BTR_j\omega_c^2C_j^2R_s}/\gamma \approx 1$ pW/$\sqrt{\mathrm{Hz}}$ at 95 GHz. Taking into account reflection loss from impedance mismatch only, the extrinsic NEP is given by $\mathrm{NEP}_e = \mathrm{NEP}_i/\eta$ where $\eta = 1 - |\Gamma|^2$ with Γ the reflection coefficient. For example, when connected to a 75 Ω load, the extrinsic NEP yields 4.7 pW/$\sqrt{\mathrm{Hz}}$ at $\omega_c/2\pi = 95$ GHz. The best NEP at 100 Hz is obtained at $V = 0$ as the rapid onset of the $1/f$ noise overwhelms the increase in the responsivity at small positive bias. The NEP values can be compared with those obtained with room temperature antenna coupled microbolometers, where the best demonstrated intrinsic NEP is about 10 pW/$\sqrt{\mathrm{Hz}}$, but can only be obtained at a modulation frequency of 50 kHz [13]. It should be noted that due to their purely real impedance, bolometers can be easily matched and have an intrinsic NEP that is independent of operating frequency.

4. THz measurements

The ever-growing interest in sensitive detectors in the THz frequencies lead us to investigate whether rectification can be observed at these frequencies which lie well above the R_jC_j rolloff of the diodes. The THz source was a far-IR cavity, pumped by a 15 W CO_2 laser. The output power of the far-IR laser was approximately 8 mW at the 2.52 THz methanol line. A mylar beam splitter was placed in the far-IR beam to couple a fraction of the power to a pyroelectric detector for real-time power monitoring. After the beam splitter, an $F/1$ off-axis paraboloid with a focal length of 25.4 mm was used to focus the far-IR power onto the diode. The diode was mounted on a 50 μm thick mylar membrane spanning a 2.75 mm diameter hole in a printed circuit board. Aluminum wire bonds from the PCB were used for the electrical connections. It is likely that at least part of the bond wires and pads serve to couple the THz to the diode. The maximum observed signal across the diode was small, $\approx 2\ \mu$V. A large amount of power is not coupled as the diode active area is likely orders of magnitude smaller than the $\pi(1.22\lambda)^2$ area of the beam.

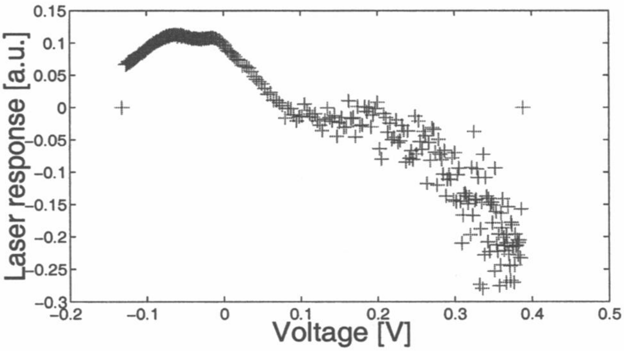

Fig. 2. Measured laser response at 2.5 THz.

The diode's THz response was also measured as a function of applied bias to determine whether or not the laser signal follows the responsivity curve determined from the $IV - dI/dV$ measurements. The measured laser response is shown in Fig. 2, where a signal is present at zero bias, a clear indication of rectification. However, there seems to be no agreement with γ (Fig. 1c). We are currently investigating the qualitative disagreement of the predicted and measured laser curves to see whether a combined bolometric and diode response might yield better fit.

5. Conclusions

We have measured the noise properties of zero bias quantum tunneling diodes and shown that these non-optimized devices have already reached a sensitivity that challenges other existing room temperature detectors in this wavelength range. The high sensitivity, low cost and reproducibility of the diodes make them an attractive newcomer to the millimeter and submillimeter-wave detector arena. The absence of $1/f$ noise and the resulting excellent narrow band NEP of the zero bias diodes can be used to its full potential in, for example, active detection where the signal is narrow band. For passive detection of thermal sources, the broadband matching poses a fundamental challenge which can be addressed by significant reduction in the junction resistance and capacitance in future devices. Rectification was observed at 2.5 THz, yet the bias dependence of the response did not agree with the DC measurements.

Acknowledgments

The authors would like to thank Aaron Miller for useful discussions.

References

1. L. Yujiri, H. Agravante, M. Biedenbender, G. Dow, M. Flannery, S. Fornaca, B. Hauss, R. Johnson, R. Kuroda, K. Jordan, P. Lee, D. Lo, B. Quon, A. Rowe, T. Samec, M. Shoucri, K. Yokoyama, and J. Yun, "Passive millimeter-wave camera," in *Passive Millimeter-Wave Imaging Technology* (R. M. Smith, ed.), vol. 3064, (Bellingham, Washington 98227-0010 USA), pp. 15–22, SPIE, SPIE, 1997.
2. T.-L. Hwang, S. Schwarz, and D. Rutledge, "Microbolometers for infrared detection," *Appl. Phys. Lett*, vol. 34, no. 11, pp. 773–776, 1979.
3. M. E. MacDonald and E. N. Grossman, "Niobium microbolometers for far-infrared detection," *IEEE Trans. Microwave Theory Tech.*, vol. 43, pp. 893–896, April 1995.
4. A. Luukanen and V.-P. Viitanen, "Terahertz imaging system based on antenna-coupled microbolometers," in *Proc. SPIE Vol. 3378, p. 34-44, Passive Millimeter-Wave Imaging Technology II, Roger M. Smith; Ed.*, pp. 34–44, Aug. 1998.
5. J. Schulman and D. Chow, "Sb-heterostructure interband backward diodes," *IEEE Electron Device Letters*, vol. 21, pp. 353–355, July 2000.
6. J. N. Schulman, D. H. Chow, E. T. Croke, C. W. Pobanz, H. L. Dunlap, and C. D. Haeussler, "Sb-heterostructure zero-bias diodes for direct detection beyond 100 GHz," in *Proc. SPIE Vol. 4111, p. 221-226, Terahertz and Gigahertz Electronics and Photonics II, R. Jennifer Hwu; Ke Wu; Eds.*, pp. 221–226, Dec. 2000.
7. J. Schulman, D. Chow, and D. Jang, "Ingaas zero bias backward diodes for millimeter wave direct detection," *IEEE Electron Device Letters*, vol. 22, pp. 200–202, May 2001.
8. R. G. Meyers, P. Fay, J. N. Schulman, S. Thomas, III, D. H. Chow, Y. K. Boegeman, J. Zinck, and P. Deelman, "Bias and temperature dependence of sb-based heterostructure millimeter wave detectors with improved sensitivity," *IEEE Electron Device Letters*, vol. 25, pp. 4–6, Jan 2004.
9. S. Ng and C. Surya, "Theory and experiments on flicker noise in $In_{0.53}Ga_{0.47}As/AlAs/InAs$ resonant tunneling diodes," *J. Appl. Phys.*, vol. 73, pp. 7504–7508, June 1993.
10. P. Fay, J. Schulman, S. Thomas III, D. Chow, Y. Boegeman, and K. Holabird, "Performance and modeling of antimonide-based heterostructure backward diodes for millimeter-wave detection," in *IEEE Lester Eastman Conference on High Performance Devices*, pp. 334–342, IEEE, Aug 2002.
11. I. Bahl and P. Bhartia, *Microwave solid state circuit design*, ch. 11, pp. 541–549. New York: John Wiley & Sons, 1988.
12. J. Schulman, V. Kolinko, M. Morgan, C. Martin, J. Lovberg, S. Thomas, III, J. Zinck, and Y. Boegeman, "W-band direct detection circuit performance with sb-heterostructure diodes," *IEEE Microwave and Wireless Component Letters*, vol. 14, pp. 316–318, July 2004.
13. A. Luukanen, *High performance microbolometers and microcalorimeters: from 300 K to 100 mK*. PhD thesis, University of Jyväskylä, Department of Physics, P.O. Box 35 (YFL) , FIN-40014 University of Jyväskylä, Finland, May 2003. http://www.phys.jyu.fi/theses/arttu_luukanen.pdf.